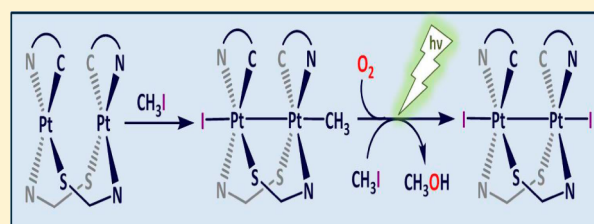


Oxidation of Half-Lantern Pt₂(II,II) Compounds by Halocarbons. Evidence of Dioxygen Insertion into a Pt(III)–CH₃ BondV. Sicilia,^{*,†} M. Baya,[‡] P. Borja,[‡] and A. Martín[‡][†]Departamento de Química Inorgánica, Escuela de Ingeniería y Arquitectura de Zaragoza, Instituto de Síntesis Química y Catálisis Homogénea (ISQCH), CSIC - Universidad de Zaragoza, Campus Río Ebro, Edificio Torres Quevedo, 50018 Zaragoza, Spain[‡]Departamento de Química Inorgánica, Facultad de Ciencias, Instituto de Síntesis Química y Catálisis Homogénea (ISQCH), CSIC - Universidad de Zaragoza, Pedro Cerbuna 12, 50009 Zaragoza, Spain

Supporting Information

ABSTRACT: The half-lantern compound $[\{\text{Pt}(\text{bzq})(\mu\text{-N}^{\wedge}\text{S})\}_2]$ (**1**) [bzq = benzo[*h*]quinoline, $\text{HN}^{\wedge}\text{S}$ = 2-mercaptopyrimidine ($\text{C}_4\text{H}_3\text{N}_2\text{HS}$)] reacts with CH_3I and haloforms CHX_3 ($\text{X} = \text{Cl}, \text{Br}, \text{I}$) to give the corresponding oxidized diplatinum(III) derivatives $[\{\text{Pt}(\text{bzq})(\mu\text{-N}^{\wedge}\text{S})\text{X}\}_2]$ ($\text{X} = \text{Cl}$ **2a**, Br **2b**, I **2c**). These compounds exhibit half-lantern structures with short intermetallic distances (~ 2.6 Å) due to Pt–Pt bond formation. The halogen abstraction mechanisms from the halocarbon molecules by the Pt₂(II,II) compound **1** were investigated. NMR spectroscopic evidence using labeled reagents support that in the case of $^{13}\text{CH}_3\text{I}$ the reaction initiates with an oxidative addition through an $\text{S}_{\text{N}}2$ mechanism giving rise to the intermediate species $[\text{I}(\text{bzq})\text{Pt}(\mu\text{-N}^{\wedge}\text{S})_2\text{Pt}(\text{bzq})(^{13}\text{CH}_3)]$. However, with haloforms the reactions proceed through a radical-like mechanism, thermally (CHBr_3 , CHI_3) or photochemically (CHCl_3) activated, giving rise to mixtures of species $[\text{X}(\text{bzq})\text{Pt}(\mu\text{-N}^{\wedge}\text{S})_2\text{Pt}(\text{bzq})\text{R}]$ (**3a–c**) and $[\text{X}(\text{bzq})\text{Pt}(\mu\text{-N}^{\wedge}\text{S})_2\text{Pt}(\text{bzq})\text{X}]$ (**2a–c**). In these cases the presence of O_2 favors the formation of species **2** over **3**. Transformation of **3** into **2** was possible upon irradiation with UV light. In the case of $[\text{I}(\text{bzq})\text{Pt}(\mu\text{-N}^{\wedge}\text{S})_2\text{Pt}(\text{bzq})(^{13}\text{CH}_3)]$ (**3d**), in the presence of O_2 the formation of the unusual methylperoxo derivative $[\text{I}(\text{bzq})\text{Pt}(\mu\text{-N}^{\wedge}\text{S})_2\text{Pt}(\text{bzq})(\text{O–O–}^{13}\text{CH}_3)]$ (**4d**) was detected, which in the presence of $^{13}\text{CH}_3\text{I}$ rendered the final product $[\{\text{Pt}(\text{bzq})(\mu\text{-N}^{\wedge}\text{S})\text{I}\}_2]$ (**2c**) and $^{13}\text{CH}_3\text{OH}$.



1. INTRODUCTION

Oxidative-addition (OA) of a molecule AB to unsaturated transition metal complexes has been widely studied as model for many catalytic reactions.^{1–3} OA to d^8 mononuclear complexes sometimes proceeds through a concerted cis addition,⁴ or through a radical-like mechanism.^{5,6} However, these reactions very often follow an $\text{S}_{\text{N}}2$ pathway,^{7–11} with the metal center acting as nucleophile through the filled d_z^2 orbital. In addition, Puddephatt and Canty have shown that OA to Pt(II) complexes of planar diimines follow a binuclear stepwise mechanism, with two π –stacked units involved in the initial oxidation step,^{12,13} providing evidence of the role of metallophilic interactions on the chemical reactivity of mononuclear d^8 complexes.

In dinuclear complexes the mechanism of OA reactions depends on many factors such as the metal, the ligands, or the nature of the AB molecule. Moreover, the possible actuation of cooperative effects between the two adjacent metals can potentially have lower activation barriers and lead to reaction pathways and products that are unable to be obtained from the mononuclear ones.^{14–18} Most usual haloalkanes, such as CH_3I and CH_2I_2 , are often added to Ir₂(I,I) via a bimetallic $\text{S}_{\text{N}}2$ pathway,^{19–21} yielding metal–metal bonded Ir(II)–Ir(II) compounds. Sometimes these reactions follow a radical-like^{22,23} mechanism or a monometallic $\text{S}_{\text{N}}2$ pathway resulting, in the latter case, in mixed valence Ir(I)–Ir(III) compounds.^{24,25}

Few examples of OA of chloroalkanes (RCl) to Ir₂(I,I) compounds leading to metal–metal bonded complexes containing Cl–Ir(II)–Ir(II)X ($\text{X} = \text{R}, \text{Cl}$) frameworks have been reported,^{26,27} and in most cases they require visible- or UV-light irradiation. Recently the OA of RCl to $[\{\text{Ir}(\mu\text{-Pz})(\text{CNBut})_2\}_2]$ ($\text{R} = \text{CH}_2\text{COMe}, \text{CH}_2\text{CO}_2\text{Me}, \text{CH}(\text{Me})\text{CO}_2\text{Me}$)²⁸ and $[\{\text{Ir}(\mu\text{-NH}_2)(\text{cod})_2\}_2]$ ($\text{RCl} = \text{CH}_2\text{Cl}_2, \text{CH}_3\text{Cl}$)²⁹ in the dark under argon atmosphere, which renders the asymmetric metal–metal bonded Ir₂(II,II) compounds, has been reported. The Ir₂(II,II) systems show relative inertness for further OA of haloalkanes, but when this occurs they render Ir₂(III,III) compounds with no metal–metal bond. Examples are illustrated by the double OA of CH_3I to complexes $[(\text{L})_2\text{Ir}(\mu\text{-Pz})_2\text{Ir}(\text{CNBut})_2]$ ³⁰ or ClCH_2R ($\text{R} = \text{Ph}, \text{CH}=\text{CH}_2$) to $[\{\text{Ir}(\mu\text{-Pz})(\text{CNBut})_2\}_2]$.²⁸

In the chemistry of binuclear Pt(II) complexes, OA reactions have been scarcely studied. OA of CH_3I (in excess) to $[\text{Pt}_2\text{Me}_2(\text{C}^{\wedge}\text{N})_2(\mu\text{-P}^{\wedge}\text{P})]$ [$\text{C}^{\wedge}\text{N}$ = 2-phenylpyridyl-H, benzo[*h*]quinoline; $\text{P}^{\wedge}\text{P}$ = dppf (1,1'-bis(diphenylphosphino)-ferrocene), dppe (1,1'-bis(diphenylphosphino)ethylene)]^{31–33} or *cis,cis*-[$\text{Me}_2\text{Pt}(\mu\text{-NN})(\mu\text{-dppm})\text{PtMe}_2$] (NN = phthalazine, dppm = bis(diphenylphosphino)methane)³⁴ takes place in two steps via a monometallic $\text{S}_{\text{N}}2$ mechanism to give the diplatinum-

Received: April 14, 2015

Published: July 21, 2015

(IV) derivatives $[\text{Pt}_2\text{Me}_4\text{I}_2(\text{C}^{\wedge}\text{N})_2(\mu\text{-P}^{\wedge}\text{P})]$ and $[\text{Me}_3\text{Pt}(\mu\text{-I})_2(\mu\text{-dppm})\text{PtMe}_3]$. In rigid metal fragments, such as lantern-shaped $\text{Pt}_2(\text{II},\text{II})$ compounds with relatively short Pt–Pt separation, the OA of halogens (X_2) or CH_3I seem to follow a bimetallic $\text{S}_{\text{N}}2$ pathway to give the corresponding metal–metal bonded $\text{Pt}_2(\text{III}–\text{III})$ complexes.^{35–37}

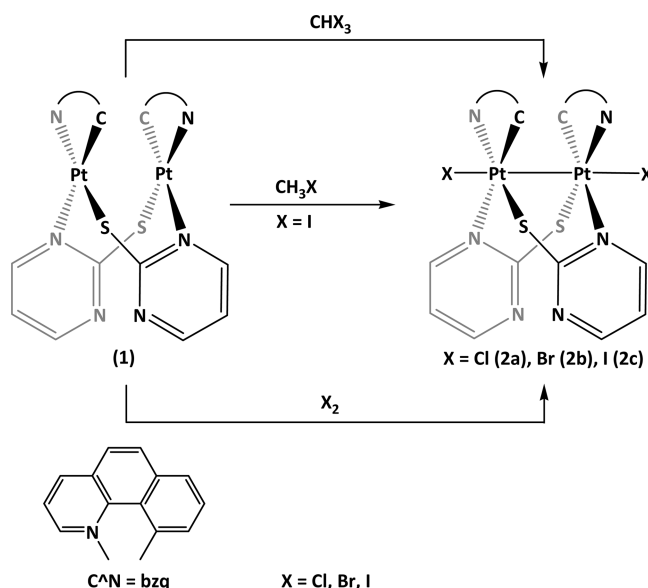
In general, lantern- or half-lantern dihalodiplatinum(III) complexes $\text{Pt}_2(\text{III}–\text{III})\text{X}_2$ ($\text{X} = \text{Cl}, \text{Br}, \text{I}$) seem to be quite stable and available by several ways, as the reaction of the corresponding $\text{Pt}_2(\text{II},\text{II})$ derivatives with halogens (X_2)^{38–40} or with an excess of RX . This behavior is illustrated by complexes $[\text{Pt}_2(\kappa^2\text{As}, \text{C}–\text{C}_6\text{H}_3\text{-5-Me-2-AsPh}_2)_2(\mu\text{-}\kappa\text{As}, \kappa\text{C}–\text{C}_6\text{H}_3\text{-5-Me-2-AsPh}_2)_2]$ and $[\text{Pt}_2(\mu\text{-}\kappa\text{As}, \kappa\text{C}–\text{C}_6\text{H}_3\text{-5-Me-2-AsPh}_2)_4]$, which in CH_2Cl_2 solution and more rapidly in CHCl_3 or CCl_4 render compound $[\text{Pt}_2\text{Cl}_2(\mu\text{-}\kappa\text{As}, \kappa\text{C}–\text{C}_6\text{H}_3\text{-5-Me-2-AsPh}_2)_4]$,⁴¹ and complex $[\text{Pt}_2\text{I}_2(\mu\text{-}\kappa\text{As}, \kappa\text{C}–\text{C}_6\text{H}_3\text{-5-Me-2-AsPh}_2)_4]$, which resulted from the reaction of $[\text{Pt}_2(\mu\text{-}\kappa\text{As}, \kappa\text{C}–\text{C}_6\text{H}_3\text{-5-Me-2-AsPh}_2)_4]$ with CH_3I in the dark.⁴¹ Other $\text{Pt}_2(\text{III},\text{III})\text{X}_2$ complexes such as $[\text{Pt}_2\text{Cl}_2(\text{pyt})_4]$ ($\text{Hpyt} = \text{pyridine-2-thiol}$)⁴² and $[\text{Pt}_2\text{Cl}_2(\text{ppy})_2(\text{pyt})_2]$ ($\text{Hppy} = 2\text{-phenylpyridine}$)⁴³ resulted from chloroform solutions of the corresponding $\text{Pt}_2(\text{II},\text{II})$ ones and mixtures of $[\text{Pt}(\text{pop})_4\text{RI}]^4$ and $[\text{Pt}(\text{pop})_4\text{I}_2]^4$ were obtained from the thermal reaction of $[\text{Pt}(\text{pop})_4]^4$ with RI ($\text{pop} = \text{pyrophosphite}$, $\text{R} = \text{Et}, \text{Pr}, \text{Pr}, n\text{-pentyl}$).⁴⁴ In spite of the surprising behavior of lantern- or half-lantern $\text{Pt}(\text{II})$ complexes toward haloalkanes (RX), studies aiming to explain the mechanism by which the $\text{Pt}_2(\text{II},\text{II})$ complexes convert into $\text{Pt}_2(\text{III}–\text{III})\text{X}_2$ are scarcely reported.⁴⁴

In the course of our research on half-lantern $\text{Pt}_2(\text{II},\text{II})$ complexes and their two-center two-electron $[2c, 2e]$ oxidation products, we prepared the new compound, $[\{\text{Pt}(\text{bzq})(\mu\text{-N}^{\wedge}\text{S})\}_2]$ (**1**) [$\text{bzq} = \text{benzo}[h]\text{quinoline}$, $\text{HN}^{\wedge}\text{S} = 2\text{-mercapto-pyrimidine}$ ($\text{C}_4\text{H}_3\text{N}_2\text{HS}$)], which reacts with excess of haloalkanes (CHCl_3 , CHBr_3 , CHI_3 , and CH_3I) to give the dihalocomplexes $[\{\text{Pt}(\text{bzq})(\mu\text{-N}^{\wedge}\text{S})\text{X}\}_2]$ ($\text{X} = \text{Cl}, \text{Br}, \text{I}$), and the reaction paths were investigated. The $\text{Pt}_2(\text{III},\text{III})\text{X}_2$ complexes were also available by treatment of **1** with halogens.

2. RESULTS AND DISCUSSION

2.1. Reactivity of a New Half-Lantern $\text{Pt}_2(\text{II},\text{II})$ Compound toward Haloforms. Synthesis of New $\text{Pt}_2(\text{III},\text{III})\text{X}_2$ Compounds ($\text{X} = \text{Cl}, \text{Br}, \text{I}$). The new half-lantern $\text{Pt}_2(\text{II},\text{II})$ complex $[\{\text{Pt}(\text{bzq})(\mu\text{-N}^{\wedge}\text{S})\}_2]$ (**1**, Scheme 1) was obtained in good yield (84%) from equimolar amounts of $[\text{Pt}(\text{bzq})(\text{NCMe})_2]\text{ClO}_4$ and $\text{HN}^{\wedge}\text{S}$ in the presence of NEt_3 . The dinuclear nature of **1** was inferred from its mass spectrum and supported by the diffusion coefficient value, which was determined using diffusion-ordered ^1H -RMN spectroscopy (DOSY) in solution (see Experimental Section in Supporting Information). The ^1H NMR spectrum of **1** indicates that it exists as a single and symmetric isomer, most probably the anti one, as observed in the related half-lantern compounds $[\{\text{Pt}(\text{bzq})(\mu\text{-C}_7\text{H}_4\text{NYS-}\kappa\text{N},\text{S})\}_2]$ ($\text{C}_7\text{H}_4\text{NYS} = 2\text{-mercaptobenzothiazolate}$ ($\text{Y} = \text{S}$); $2\text{-mercaptobenzoxazolate}$ ($\text{Y} = \text{O}$)).^{39,40} As with the aforementioned compounds,^{39,40} the electronic absorption spectra of **1** (Figure S1 in Supporting Information) show low-intensity bands centered at 496 nm (CH_2Cl_2) or 580 nm (powdered solid), assignable to a metal–metal-to-ligand charge transfer transition, ($^1\text{MMLCT}$) $[\text{d}\sigma^*(\text{Pt})_2 \rightarrow \pi^*(\text{bzq})]$, which is indicative of the existence of two platinum centers located in close proximity, both in the solid state and in solution. Unlike them, complex **1** is not emissive upon excitation at wavelengths from 350 to 580 nm at either 298 or 77 K.

Scheme 1. Reactions Leading to $\text{Pt}_2(\text{III},\text{III})\text{X}_2$ (**2a–2c**) from $\text{Pt}_2(\text{II},\text{II})$ (**1**)



Complex **1** readily reacts with an excess of haloforms, CHX_3 ($\text{X} = \text{Cl}, \text{Br}, \text{I}$), in the air, to give the corresponding $\text{Pt}_2(\text{III},\text{III})\text{X}_2$ complexes $[\{\text{Pt}(\text{bzq})(\mu\text{-N}^{\wedge}\text{S})\text{X}\}_2]$ ($\text{X} = \text{Cl}$ **2a**, Br **2b**, I **2c**), which were isolated as pure compounds (Scheme 1). The reactions with CHBr_3 and CHI_3 proceed in the dark to give **2b** and **2c**, respectively, which were isolated in ca. 60% yield after 24 h (see Experimental Section in Supporting Information). However, in CHCl_3 solution compound **1** is stable in the dark, but in the sunlight it reacts with CHCl_3 to render complex **2a** that was obtained in 88% yield after 6 h (see Experimental Section in Supporting Information).

The same oxidized complexes were also obtained upon treatment of **1** with the corresponding halogen X_2 (see Scheme 1 and Experimental Section in Supporting Information). All these $\text{Pt}_2(\text{III},\text{III})\text{X}_2$ compounds show a half-lantern structure with short Pt–Pt distances (2.6132(2) Å **2a**, 2.6167(4) Å **2b**, 2.6401(2) Å **2c**), in agreement with the existence of a Pt–Pt bond (see Figure 1 for **2c**, Figure S3 in Supporting Information for **2a** and **2b** and Table S3 in Supporting Information). Their structures are similar to those observed for compounds $[\{\text{Pt}(\text{bzq})(\mu\text{-C}_7\text{H}_4\text{NYS-}\kappa\text{N},\text{S})\text{X}\}_2]$ ($\text{Y} = \text{S}, \text{O}$; $\text{X} = \text{Cl}, \text{Br}, \text{I}$).^{39,40} In all of them, the $\text{Pt}(\text{III})$ centers have distorted octahedral environments with the axial positions occupied by a halogen atom and the other $\text{Pt}(\text{III})$ center; the $\text{X}–\text{Pt}–\text{Pt}$ angles are close to 175° . The Pt–Pt distances are similar to those observed in $[\text{Pt}_2\text{Cl}_2(\text{ppy})_2(\text{pyt})_2]$ ⁴³ and shorter than those observed in compounds $[\{\text{Pt}(\text{bzq})(\mu\text{-C}_7\text{H}_4\text{NYS-}\kappa\text{N},\text{S})\text{X}\}_2]$ ($\text{Y} = \text{S}, \text{O}$).^{39,40} This fact must be related with the value of the $\text{N}–\text{C}–\text{S}$ bond angle of the bridging ligand, which is smaller in **2a–2c** ($\sim 121^\circ$) than in complexes $[\{\text{Pt}(\text{bzq})(\mu\text{-C}_7\text{H}_4\text{NYS-}\kappa\text{N},\text{S})\text{X}\}_2]$ ($\text{Y} = \text{S}, \sim 128^\circ$ or $\text{O}, \sim 130^\circ$).

In all these $\text{Pt}_2(\text{III},\text{III})\text{X}_2$ compounds the platinum coordination planes are almost parallel, with interplanar angles close to 10° ($7.58(5)^\circ$ **2a**, $9.31(13)^\circ$ **2b**, 9.20° **2c**). Angles between the Pt–Pt line and the normal lines to the Pt coordination planes are small too, the biggest one being $5.12(9)^\circ$ (for compound **2b**). These structures exhibit significant intramolecular $\pi–\pi$ interactions between the bzq groups, with most C–C distances between 3.19 and 3.99 Å (**2a**), 3.26 and 3.98 Å (**2b**), and 3.18 and

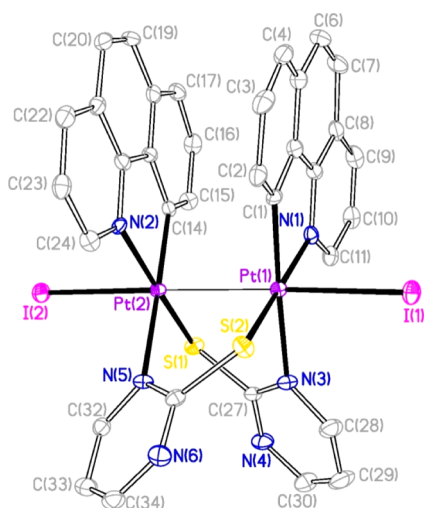
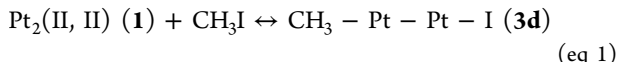


Figure 1. Molecular structure of **2c**. Ellipsoids are drawn at their 50% probability level; solvent molecules and hydrogen atoms were omitted for clarity.

3.99 Å (**2c**).^{39,40,45–48} Complexes **2a–2c** are discrete molecules, and no intermolecular interactions between neighbor molecules were found.

2.2. Reactivity of 1 toward CH₃I. Formation of Compound Pt₂(III,III)I₂ (2c**).** We observed that complex **1** reacts with an excess of CH₃I (molar ratio 1:3.65) in the dark within 8 min to render the new species [I(bzq)Pt(μ-N[^]S)₂Pt(bzq)(CH₃)](**3d**), which in the sunlight evolves to **2c** (Scheme 2). Compound **2c** can be directly obtained by reaction of **1** with CH₃I (molar ratio 1:4) in the air and in the sunlight in moderate yield (see Scheme 1 and Experimental Section in Supporting Information). However, in the dark, **3d** has been proven to be stable for at least 22 h.

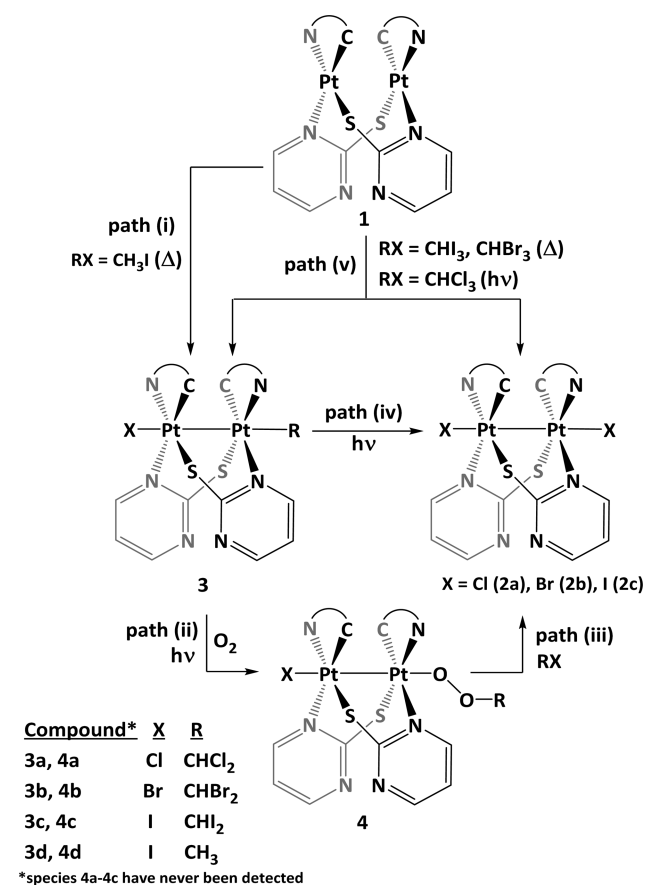
Attempts to isolate **3d** as a pure solid from the reaction crude in different solvents and temperatures were unsuccessful, and mixtures of **3d**, **1**, and free CH₃I were always obtained. These observations suggest that the reaction of **1** with CH₃I is an equilibrium (see eq 1), which would explain that the evaporation of the volatile CH₃I forces the equilibrium to the left, therefore regenerating **1**. This equilibrium happens to be very sensitive to the temperature, in a way that the formation of **1** and CH₃I from **3d** was observed by NMR when the temperature increases over 30 °C. Poor-quality crystals of **3d** were eventually obtained from these reaction mixtures that enabled to establish the connectivity of the atoms, which confirmed the proposed structure for **3d** (Figure S4 in Supporting Information).



The reaction mechanisms for the formation of Pt₂(III,III)X₂ (X = Cl **2a**, Br **2b**, I **2c**) from **1** and an excess of halocarbons (CHX₃, CH₃I) were investigated. For a better understanding, the results obtained for the reaction of **1** with CH₃I are described first.

2.3. Mechanism Insight for the Reaction of 1 with CH₃I. Evidence of Dioxygen Insertion into a Pt(III)–CH₃ Bond. The reaction of **1** with ¹³CH₃I (molar ratio 1:3.65) was studied by multinuclear NMR spectroscopy in CD₂Cl₂, including two-dimensional techniques (¹H COSY and ¹H, ¹³C HSQC). These studies showed that **1** reacts quickly with ¹³CH₃I in the air and in the dark at room temperature to give the new species

Scheme 2. Mechanism Proposed for the Oxidation of **1** with Halocarbons



[I(bzq)Pt(μ-N[^]S)₂Pt(bzq)(¹³CH₃)] (**3d**) (Figure 2 and Scheme 2).

The ¹H NMR spectrum of **3d** shows a doublet at 1.02 ppm corresponding to the ¹³CH₃ fragment with a ¹J_{C–H} = 139 Hz. This signal is flanked by two sets of ¹⁹⁵Pt satellites (²J_{Pt–H} = 55 Hz, ³J_{Pt–H} = 15 Hz) with the ⁿJ_{Pt–H} values (*n* = 2, 3) being similar to those reported by H. B. Gray et al. for the full-lantern compound K₄[Pt₂(pop)₄(CH₃)I] (²J_{Pt–H} = 52.66 Hz, ³J_{Pt–H} = 13.83 Hz).³⁵ Moreover, the ¹³C {¹H} NMR spectrum shows a singlet at 3.78 ppm flanked by two sets of ¹⁹⁵Pt satellites (¹J_{Pt–C} = 453 Hz, ²J_{Pt–C} = 160 Hz), also consistent with a dinuclear Pt₂(III,III) formulation with the CH₃ and I ligands in the axial positions.

Interestingly, when this reaction sample containing [I(bzq)Pt(μ-N[^]S)₂Pt(bzq)(¹³CH₃)] (**3d**) and ¹³CH₃I was irradiated with UV light (λ = 365 nm) for 1 h, new signals corresponding to three new species emerged (see Figure 3): [I(bzq)Pt(μ-N[^]S)₂Pt(bzq)(O–O¹³CH₃)] (**4d**), **2c**, and ¹³CH₃OH (δH = 3.40 ppm (d), ¹J_{C–H} = 142 Hz; δC = 50.8 ppm (s)). Species **4d** is a new platinum complex whose ¹H and ¹³C NMR spectra exhibit the signals due to ¹³CH₃ with no coupling to ¹⁹⁵Pt (δH = 2.45 ppm (d), ¹J_{C–H} = 140 Hz; δC = 64.2 ppm (s)). The values of ¹J_{C–H} and δC,^{49,50} together with the absence of Pt–¹³C and Pt–H couplings, lead us to propose **4d** to be a methylperoxo^{48,51,52} over a methoxo^{53–58} species as represented in Scheme 2. The ¹H NMR signal corresponding to ¹³CH₃OO (δH = 2.45 ppm) for **4d** appears highfield-shifted with respect to those in the mononuclear Pt(II) methylperoxo (δH > 3.0 ppm) derivatives previously described.^{49,51,52}

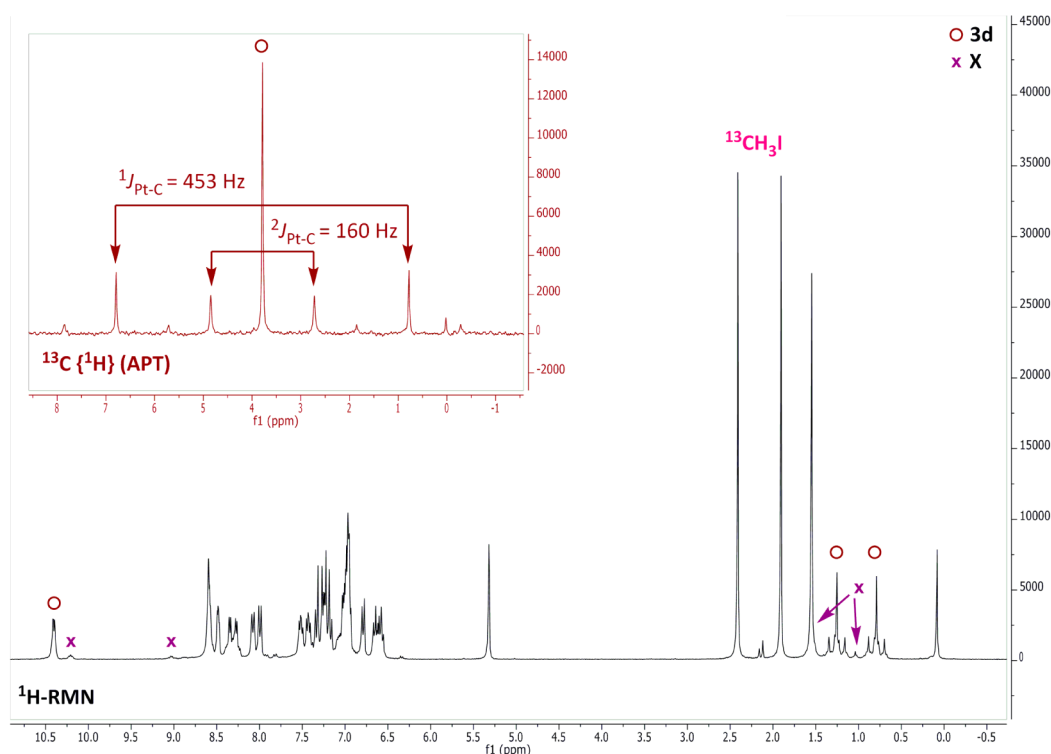


Figure 2. ^1H NMR spectrum of the reaction of **1** with $^{13}\text{CH}_3\text{I}$ (1:3.65) in CD_2Cl_2 in the air and in the dark after 8 min. (inset) Expansion of the $\text{Pt}-^{13}\text{CH}_3$ signal of **3d** in the $^{13}\text{C}\{^1\text{H}\}$ NMR spectrum (APT).

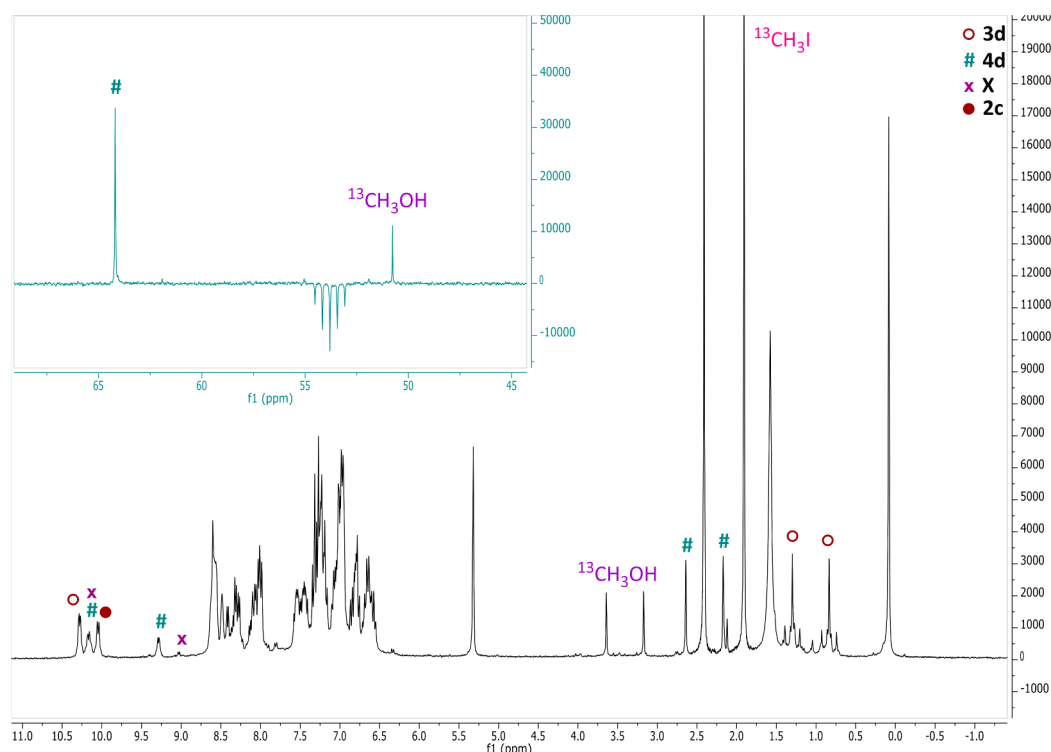


Figure 3. ^1H NMR spectra of the reaction of **1** with $^{13}\text{CH}_3\text{I}$ (1:3.65) in CD_2Cl_2 when exposed for 1 h to UV light ($\lambda = 365$ nm). (inset) $^{13}\text{C}\{^1\text{H}\}$ (APT) expansion of the new signals observed (**4d** and MeOH).

A comparable shift was observed in the Pt(IV) methoxy complexes, $\text{fac-[PtMe}_2(\text{OMe})(\text{D}_2\text{O})_3]\text{NO}_3$ ($\delta\text{H}(\text{OMe}) = 2.43$ ppm),⁵⁸ and $[\text{Pt}(\text{OH})(\text{OCH}_3)\text{Me}_2(\text{bipy})]$,⁵⁵ which suggests that the oxidation state of the metal atom could affect the δH value of the CH_3OO fragment. However, in our case, it is

probably due to the anisotropic shielding effect of the aromatic ring current of **bzq** on these hydrogen atoms lying close to it. When the same sample was irradiated with UV light for 12 additional hours, species **3d** and **4d** were completely transformed into **2c** (path iii, Scheme 2), whereby the amount of $^{13}\text{CH}_3\text{OH}$ in

the mixture was increased. The integrals of the ^1H signals indicate $2\text{c}/^{13}\text{CH}_3\text{OH} \approx 1:2$, and no other oxygenated organic species, such as formaldehyde, were detected.

Under Ar atmosphere, complex **1** also reacts readily with CH_3I (molar ratio 1:3.65) in the dark at room temperature to give the asymmetric species **3d**. When this sample containing **3d** and excess of CH_3I was exposed to the UV light, only 26% of **3d** appeared quantitatively transformed into **2c** after 3 d, and species **4d** and CH_3OH were not detected during this time, in agreement with the absence of molecular oxygen in the environment. This observation proved that there is an additional “oxygen-free” pathway for the conversion of **3d** into the diiodide complex **2c** (path iv in Scheme 2). Nevertheless, the presence of molecular oxygen provides a faster and more efficient conversion pathway into **2c** (paths ii and iii, Scheme 2).

The above presented data support that the formation of **2c** from **1** and CH_3I follows a stepwise mechanism. The first step consists in the thermal OA of CH_3I to **1** to give **3d** (path (i)). Subsequently the photochemical transformation of **3d** into **2c** may occur through two alternative pathways, with or without oxygen (paths ii and iii or path iv, respectively, in Scheme 2). To get a deeper knowledge of this mechanism, we decided to check whether radicals might be involved in the first (path (i)) and second steps (paths ii and iv, Scheme 2) of the reaction, by testing the effect of a typical radical reagent as galvinoxyl (Gal^\bullet). We did not exclude path (i) from this study, keeping in mind that thermal OA can take place not only through an $\text{S}_\text{N}2$ but also through a radical-like mechanism, as for instance in the reported OA of alkyl iodides to $[\text{Pt}_2(\text{pop})_4]^{4-44}$ and $[\text{PtMe}_2(\text{phen})]$ (phen = 1,10-phenanthroline).⁵⁹ However, the need for irradiation to reach the transformation of **3d** into **2c** (paths ii and iv) is not an unambiguous sign of a radical-based mechanism, as it occurs in complex $[\text{Pt}(\text{CH}_3)(\text{N}^\wedge\text{N}^\wedge\text{N})](\text{SbF}_6)$ ($\text{N}^\wedge\text{N}^\wedge\text{N}$ = 6,6'-diaminoterpyridine).⁴⁹

Two comparative experiments with and without Gal^\bullet showed that in both cases **1** reacts with $^{13}\text{CH}_3\text{I}$ readily in the dark to give species **3d**. As no diamagnetic species, arising from coupling of Gal^\bullet with other generated radicals, were observed (^1H NMR) in the sample containing Gal^\bullet , it could be concluded that path (i) does not follow a radical-like mechanism but rather an $\text{S}_\text{N}2$ one. To check path ii, one set of two samples containing species **3d** and excess of $^{13}\text{CH}_3\text{I}$, with and without Gal^\bullet , was prepared in the dark and in the air and then exposed to the UV light for 10 min. An identical experiment was performed to check path iv but with the set of samples being prepared under Ar atmosphere.⁶⁰ In these experiments we observed that in the samples containing Gal^\bullet , the transformation of **3d** into **2c** was faster and that their ^1H NMR spectra showed the presence of diamagnetic species arising from coupling of Gal^\bullet with other generated radicals.

The observed effect of Gal^\bullet and the invariably required light for the transformation of **3d** into **2c** are consistent with a radical-like mechanism, both in the presence of O_2 (path ii, Scheme 2) and in the absence of it (path iv, Scheme 2). In the absence of O_2 , one possible explanation could come from the photochemical bond homolysis of the Pt– CH_3 bond⁶¹ of **3d** upon UV light irradiation; the organometallic radical would abstract I from CH_3I (preferentially than from the CD_2Cl_2 used as solvent) to give **2c**. In the presence of O_2 , an important fraction of this radical-like transformation seems to occur through the methylperoxo intermediate **4d**.

Insertion of O_2 into an M–R bond to give an alkylperoxo complex is a rare feature for a late transition metal. Very few examples of stable Pt alkylperoxide complexes have been

described, $[\text{Pt}(\text{L})\text{OOMe}][\text{SF}_6]$ (L = 6,6'-diaminoterpyridine),^{49,52} $[(\text{PN})\text{PtMe}(\text{OOMe})]$ (PN = 2-((di-*tert*-butylphosphino)methyl)pyridine)⁵¹ or $[\text{PtMe}_2(\text{NN})(\text{OOR})\text{I}]$ (NN = bpy, phen; R = 'Pr, 'Bu),⁵⁹ all of them being mononuclear complexes of Pt(II) and Pt(IV). To the best of our knowledge no dinuclear metal–metal bonded alkylperoxo complexes, like **4d**, have been reported so far. In this context, Goldberg⁵¹ has also proposed a radical mechanism for the thermal reaction of $[(\text{PN})\text{PtMe}_2]$ (PN = 2-((di-*tert*-butylphosphino)methyl)pyridine) with O_2 , in view of the effects of light and the radical inhibitor 4-methyl-2,6-di-*tert*-butylphenol on the reaction rate. The resulting complex $[(\text{PN})\text{PtMe}(\text{OOMe})]$ converts to $[(\text{PN})\text{PtMe}(\text{Cl})]$ in CD_2Cl_2 , similarly to the observed transformation of complex **4d** into **2c** in the presence of CH_3I (species **4d** has proven not to be stable in the presence of $^{13}\text{CH}_3\text{I}$ and to convert into **2c** even in the dark). These results differ from the nonradical mechanism proposed for Britovsek et al. for the light-driven insertion of O_2 into the Pt–Me bond in $[\text{Pt}(\text{L})\text{Me}][\text{SF}_6]$ (L = 6,6'-diaminoterpyridine). In this case, the effect of light seemed to be the conversion of the loosely aggregated Pt(II) complexes $[\text{Pt}(\text{II})\cdots\text{Pt}(\text{II})]$ into a triplet state $^3[\text{Pt}(\text{III})\text{–Pt}(\text{III})]^*$, which can react with $^3\text{O}_2$, rather than $^3\text{O}_2$ sensitization by the Pt(II) complex, to generate $^1\text{O}_2$ before its insertion into the Pt–Me bond.⁴⁹ The methylperoxo derivative $[\text{Pt}(\text{L})\text{OOMe}][\text{SF}_6]$ is not stable at room temperature and decomposes in acetone- d_6 in the ambient light to give $[\text{Pt}(\text{L})\text{OH}][\text{SF}_6]$ and formaldehyde.

2.4. Mechanistic Insight for the Oxidation Reaction of the Half-Lantern $\text{Pt}_2(\text{II,II})$ Complex **1 with Haloforms.** The reactions of **1** with an excess of CHX_3 (X = Cl, Br, I) rendered complexes $\text{Pt}_2(\text{III,III})\text{X}_2$ (**2a–2c**) in moderate-to-good yield, as we mentioned above. With CHBr_3 and CHI_3 they proceed in the dark, but the reaction with CHCl_3 requires light to go on.

The reaction of **1** with CHBr_3 was followed by multinuclear NMR spectroscopy using $^{13}\text{CHBr}_3$ (molar ratio 1:3.25) as reagent and CD_2Cl_2 as solvent. When the reaction sample was prepared in an NMR tube in the dark and in the air, species $[\text{Br}(\text{bzq})\text{Pt}(\mu\text{-N}^\wedge\text{S})_2\text{Pt}(\text{bzq})(^{13}\text{CHBr}_2)]$ (**3b**) and **2b** were observed (Scheme 2, path (v)) from the beginning (12 min.) in 2:1 molar ratio, together with the starting compound **1** (see Figure S5 in Supporting Information), and free $^{13}\text{CHBr}_3$ (δ_H = 6.91 ppm; δ_C = 10.31 ppm; $^1J_{\text{C–H}}$ = 206 Hz). The NMR parameters associated with the $^{13}\text{CHBr}_2$ fragment in **3b** (δ_H = 4.49 ppm (d), $^1J_{\text{C–H}}$ = 175 Hz, $^2J_{\text{Pt–H}} \approx 11$ Hz; δ_C = 20.85 ppm, $^1J_{\text{Pt–C}}$ = 623 Hz; $^2J_{\text{Pt–C}}$ = 512 Hz), are similar to those corresponding to the CH_2 unit in $[\text{Cp}(\text{acac})\text{Ti}(\mu_3\text{-S})_2\text{Ir}_2(\text{CH}_2)_2\text{I}(\text{CO})_4]$ (δ_H = 4.74 ppm (s), δ_C = 26.3 ppm),²² according with the proposed dinuclear $\text{Pt}_2(\text{III,III})$ formulation for **3b**. Compound **1** was completely transformed into **2b** (33%) and **3b** (66%) in 9.5 h. For comparative purposes, the same reaction was performed in the dark either under Ar or O_2 atmospheres (Figure S6 in Supporting Information). Both samples showed, after 2 h, mixtures of the three species (**3b**, **2b**, and **1**) but in different ratios (under Ar: **1** (35%), **2b** (17%), **3b** (48%); in O_2 : **1** (20%), **2b** (50%), **3b** (30%)). These experimental data proved that O_2 is not essential for the formation of **2b** from **1** and CHBr_3 , but it favors its formation. The direct formation of **2b** from **1** due to small amounts of Br_2 (generated by O_2) seems unlikely and can be ruled out since it occurred under Ar atmosphere. Then, the simultaneous formation of **2b** and **3b** suggests a radical pathway for the addition reaction.⁴⁴ To check this possibility we performed comparative experiments of the reaction of **1** with $^{13}\text{CHBr}_3$, both

with and without Gal[•], in the dark. After 2 h (in the air and in Ar atmospheres) the reactions in the presence of Gal[•] were slower, and the ratio of **2b** in the mixtures was bigger than in the absence of it (Supporting Information, Figure S7). All the experimental results concerning this reaction are in agreement with a radical pathway eq 2–eq 5, in which both O₂ and Gal[•] act as radical (R[•]) traps, increasing the **2b**:**3b** ratio.^{44,62}



The reaction of **1** with CHI₃ (1:2 molar ratio) in CD₂Cl₂ at room temperature in the dark was shown to proceed in the same way but faster than that with CHBr₃. In the air, compound **2c** was quantitatively formed just upon mixing the reagents, as determined by ¹H NMR. Under Ar atmosphere a mixture of species [I(bzq)Pt(μ-N[^]S)₂Pt(bzq)(CHI₂)](**3c**) and **2c** (molar ratio 6:1), with no traces of the starting compound **1**, was detected by ¹H NMR (Figure S8 in Supporting Information) in just 15 min. So, in this case, O₂ acts as an efficient radical (R[•]) trap facilitating the complete conversion of **1** into **2c** in a few minutes.

Then, we studied the possible transformation of **3b/c** into **2b/c**. As a result of several experiments, we observed that the reaction mixtures containing species **3** and **2** remained invariable in the dark as much under Ar as in the air. However, irradiation with UV light promotes this transformation, which was revealed to be faster in the air than under Ar atmosphere.

In CHCl₃ solution, compound **1** is stable in the dark at room temperature, but in the sunlight it reacts to render complex **2a** in good yield. Most photooxidations of Pt(II) complexes in halocarbons have been described as requiring UV light to occur.^{63–66} However, in our case we observed that this reaction takes place simply upon irradiation with green light-emitting diodes (LEDs, λ ≈ 500 nm). Thus, a solvent-initiated radical-like pathway could be excluded. Monitoring by UV–visible spectroscopy the decay of the MMLCT absorption of complex **1** (~495 nm in CHCl₃) when it reacts with CHCl₃ upon irradiation with green LEDs (λ ≈ 500 nm) (Table S4 and Figures S9 and S10 in Supporting Information) we could observe that the initial reaction rate increases with the concentration of nucleophile **1**. This fact is consistent with an S_N2 mechanism^{59,60,62} for the OA reaction, but it seems unlikely since complex **1** remained unreacted in refluxing CHCl₃ solution in the dark, both in the air and in Ar atmosphere.

For comparative purposes two samples containing **1** and distilled CDCl₃ as solvent and reagent were prepared in the dark, one in the air and the other one under Ar atmosphere. Their ¹H NMR spectra revealed that upon irradiation with green LEDs for 6 h the complete oxidation of **1** occurred, with **2a** being the sole species observed in the sample prepared in the air while a mixture of **2a** (15%), **3a** (70%) and unidentified species (15%) was in the other one.⁶⁷ In the presence of Gal[•] the reaction was slower than in the absence of it, and **2a** was the only oxidized species as much in the air as under Ar atmosphere. These observations are in agreement with the free radical (R[•]) trap role of Gal[•] and O₂ in this reaction.

Then, we studied the possible transformation of **3a** into **2a**. As results of several experiments we observed that the mixtures remained invariable in the dark and that upon irradiation with

green LEDs for 17 h **3a** was still present in the mixtures in ≈10%, in the air and under Ar atmospheres. Keeping in mind that irradiation of the sample containing **1** and distilled CDCl₃ in the air for 6 h rendered **2a** as the sole oxidized compound, it seems evident that **2a** should be formed directly from **1**, rather than from the slow transformation of **3a**.

Despite similarities, there is an important difference with respect to the reaction of **1** with CHX₃ (X = Br, I). While the latter proceeds in the dark, the reaction with CHCl₃ needs light to go on, indicating that it is photochemically but not thermally initiated. Given that complex **1** absorbs at 495 nm (¹MMLCT band), irradiation with green light would lead to MMLCT excited Pt₂(II,II) complexes, whose interaction with CHCl₃ will undergo dissociation into Pt₂Cl[•] and CHCl₂[•], as the first step of a radical reaction pathway.⁶⁸

2.5. Density Functional Theory Calculations for the Oxidative Addition Reaction Step, through an S_N2 Mechanism.

We found that the reactions of **1** with haloforms proceed immediately in the dark for CH₃I and CHI₃, slowly with CHBr₃, and must be photochemically initiated in the case of CHCl₃. This behavior parallels the increasing bond energy of the C–X bond (bond dissociation energies increase in the sequence C–I < C–Br < C–Cl).^{69,70} Concerning the OA step of these reactions, the one with CH₃I seems to follow a typical S_N2 pathway, whereas a radical-like mechanism seems to be operative for all the three haloforms. To obtain additional pieces of the puzzle, we performed the density functional theory (DFT) modelization of the S_N2 mechanism for the OA step, leading to the formation of the asymmetric R–Pt(III)–Pt(III)–X complexes **3**, and compared the results with the experimental data collected. Thus, we studied the gas-phase 1:1 reaction of the haloalkanes with the Pt₂(II,II) precursor **1** at the M06/SDD(f)/6-31g* level of theory (see computational details in Supporting Information). Electronic and free energies in the gas phase (Figure 4a) and free energies in CH₂Cl₂ solution (Figure 4b) computed by using the PCM model were included in the discussion. In all cases the reference energy values (0.0 kcal/mol) have been assigned to the Pt(II)–Pt(II)···R–X adducts.

In general terms the energy profiles obtained consist of potential energy curves with pre- and post-reaction intermediates separated by a central barrier (Figure 4). Similar profiles were observed in related cases modeled by DFT, as in the bimolecular S_N2 reaction X[–] + CH₃Y → XCH₃ + Y[–].⁷¹ Thus, the first step consists of the interaction of the Pt₂(II,II) precursor acting as a nucleophile with the haloalkane. The formed adduct results from the stabilizing interaction of the Pt₂-centered highest occupied molecular orbital of the dinuclear complex with the electrophilic C atom of the halogenated substrate. The next step consists of the nucleophilic substitution itself, which happens through a transition state showing a hypervalent C atom with two long Pt···C and C···X distances, which subsequently leads to the formation of a cationic Pt(II)–Pt(IV)–R intermediate stabilized by the halide anion. Finally, the migration of the halide to the Pt(II) center of the latter intermediate generates the final R–Pt(III)–Pt(III)–X derivative **3**.

The theoretical results show interesting trends that must be highlighted. From a thermodynamic point of view the formation of the R–Pt(III)–Pt(III)–X derivatives (**3**) through an S_N2 mechanism is little exothermic, with ΔG_{sol} values between –0.7 and –5.2 kcal/mol (ΔE_{gas} between +1.5 and –2.6 kcal/mol). This indicates that species **3**, directly resulting from the formal OA of the RX molecules, are just scarcely favored over the reactants. The nearly reversible character of these processes

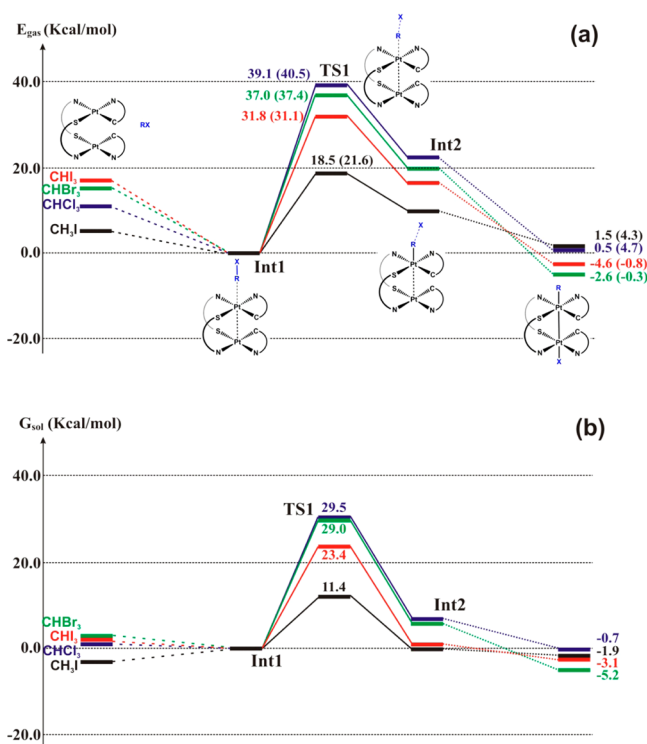


Figure 4. DFT-calculated energy profiles for the S_N2 reactions of complex **1** with haloalkanes. (a) Electronic energies and free energies (in parentheses), calculated in the gas phase. (b) Free energies, calculated in CH_2Cl_2 solution.

justifies the failure to isolate the asymmetric species **3d** as pure compound.

From the kinetic point of view, OA of CH_3I to the $\text{Pt}_2(\text{II},\text{II})$ species is rather different than the addition of the CHX_3 ($\text{X} = \text{Cl}, \text{Br}, \text{I}$) molecules. The activation energy in the former case is remarkably low ($\Delta G_{\text{sol}} = +11.4$ kcal/mol; $\Delta E_{\text{gas}} = +18.5$ kcal/mol), suggesting that this process shall readily occur through a classical S_N2 mechanism with no need of heating or light irradiation. This is in agreement with the easy and fast formation of the $\text{CH}_3\text{-Pt(III)-Pt(III)-I}$ derivative **3d** in solution. In contrast, the activation energies of the OA of the haloforms to the dinuclear precursor are markedly higher, following the order $\text{I} < \text{Br} < \text{Cl}$. At first sight, the energy barriers calculated in the gas phase may appear very high (ΔE_{gas} from +31 to +40 kcal/mol); however, correction of the solvent effects by using the polarizable continuum model (PCM) affords a decrease of these energies. Among them, the OA of iodoform shows a ΔG_{sol} activation barrier of 23.4 kcal/mol, whereas the barriers for bromoform and chloroform are 29.0 and 29.5 kcal/mol. These data suggest that the S_N2 mechanism could still be operative, simultaneously with a radical-like mechanism, for the reaction of **1** with CHI_3 , but it appears unlikely for the reactions of **1** with CHBr_3 and CHCl_3 .

Besides, the experimental data show that the reaction of the $\text{Pt}_2(\text{II},\text{II})$ species **1** with RX substrates eventually yields the symmetric $\text{X-Pt(III)-Pt(III)-X}$ (**2**) derivatives instead of the asymmetric $\text{R-Pt(III)-Pt(III)-X}$ (**3**) species. Thus, the former compounds appear to be thermodynamic sinks in the oxidation processes. Consistent with this, the oxidation of the Pt(II)-Pt(II) precursor with X_2 quickly and quantitatively affords the $\text{X-Pt(III)-Pt(III)-X}$ species **2** (see Scheme 1). To complete the picture of our DFT studies, the OA of the $\text{Pt}_2(\text{II},\text{II})$ species **1** with X_2 through an S_N2 mechanism was also modeled.

In all three cases ($\text{X} = \text{Cl}, \text{Br}, \text{I}$), the energy profiles obtained in the gas phase are simpler (Figure S11 in Supporting Information), as only one intermediate species between the reactants and products was found. DFT calculations on these oxidation processes predict very favored reactions, in agreement with the high thermodynamic stability of the $\text{Pt}_2(\text{III},\text{III})\text{X}_2$ derivatives **2**. The formation of the dihalogenated species is increasingly favored in the sequence $\text{I} < \text{Br} < \text{Cl}$ and present ΔG_{sol} values between -9 and -31 kcal/mol (ΔE_{gas} between -11 and -38 kcal/mol). These data are in obvious contrast with the barriers computed for the first series of oxidative addition processes, which are either balanced or slightly exothermic processes.

3. CONCLUSIONS

The new half-lantern compound $[\{\text{Pt}(\text{bzq})(\mu\text{-N}^{\wedge}\text{S})\}_2]$ (**1**) [$\text{bzq} = \text{benzo}[h]\text{quinoline}$, $\text{HN}^{\wedge}\text{S} = 2\text{-mercaptopyrimidine}$] has been found to promote C–X bond activation in haloforms CHX_3 ($\text{X} = \text{Cl}, \text{Br}, \text{I}$) and CH_3I . In excess of RX the reactions lead to the oxidized $\text{Pt}_2(\text{III},\text{III})\text{X}_2$ (**2a–2c**) compounds in reasonable-to-good yields. With CH_3I the reaction consists in the thermal OA of RX to the $\text{Pt}_2(\text{II},\text{II})$ complex **1** through an S_N2 mechanism, to selectively give $[\text{X}(\text{bzq})\text{Pt}(\mu\text{-N}^{\wedge}\text{S})_2\text{Pt}(\text{bzq})\text{R}]$ (**3d**). However, with the haloforms, the reactions proceed through a radical-like mechanism, thermally (CHBr_3 , CHI_3) or photochemically (CHCl_3) activated, giving rise to mixtures of species $[\text{X}(\text{bzq})\text{Pt}(\mu\text{-N}^{\wedge}\text{S})_2\text{Pt}(\text{bzq})\text{R}]$ (**3a–c**) and $[\text{X}(\text{bzq})\text{Pt}(\mu\text{-N}^{\wedge}\text{S})_2\text{Pt}(\text{bzq})\text{-X}]$ (**2a–c**) in different ratios. In these cases, O_2 acts as radical scavenger (R^{\bullet}), like Galvinoxyl, favoring the formation of species **2** over **3**. Species **3a–d** have been proved to be stable in the dark, either under Ar or in the air, but they transform into **2a–c** upon irradiation. Spectroscopic evidence supports that in the presence of O_2 the transformation of the labeled species $[\text{I}(\text{bzq})\text{Pt}(\mu\text{-N}^{\wedge}\text{S})_2\text{Pt}(\text{bzq})(^{13}\text{CH}_3)]$ (**3d**) occurs through the unusual methylperoxo derivative $[\text{I}(\text{bzq})\text{Pt}(\mu\text{-N}^{\wedge}\text{S})_2\text{Pt}(\text{bzq})(\text{O}-\text{O}^{13}\text{CH}_3)]$ (**4d**), which, in the presence of $^{13}\text{CH}_3\text{I}$, renders the final products $[\{\text{Pt}(\text{bzq})(\mu\text{-N}^{\wedge}\text{S})\}_2]$ (**2c**) and $^{13}\text{CH}_3\text{OH}$.

■ ASSOCIATED CONTENT

Supporting Information

Experimental procedures and materials. Numeration scheme for NMR purposes. Synthesis details. Diffusion-ordered ^1H -RMN spectroscopy (DOSY) in solution. Normalized absorption spectra of **1** at room temperature. X-ray structure determination and crystal data of compounds **2a–2c** and **3d**. Computational details including molecular structure of **2a**, **2b**, and **2b'**. Selected bond distances (Å) and angles (deg) of compounds **2a** and **2c**. Molecular structure of **3d**. ^1H NMR spectra of the reactions of **1** with $^{13}\text{CHBr}_3$ (1:3.25) and CHI_3 (1:2) in CD_2Cl_2 in different conditions. Initial reaction rates of the reaction of **1** with CHCl_3 . LEDs disposition in the UV–vis spectrophotometer for kinetic measurements. Absorbance–time graphic ($\lambda = 490$ nm) for the reaction of **1** with CHCl_3 under irradiation with green LEDs ($\lambda \approx 500$ nm) at 25°C . DFT-calculated energy profiles for the S_N2 reactions of X_2 and **1**. Electronic energies and free energies (in parentheses) calculated in the gas phase. Free energies calculated in CH_2Cl_2 solution. The Supporting Information is available free of charge on the ACS Publications website at DOI: 10.1021/acs.inorgchem.5b00846. CCDC Nos. 1056301–1056303 contain the supplementary crystallographic data for compounds **2a**· CH_2Cl_2 , **2b**·2THF, and **2c**·2 CH_2Cl_2 , respectively. These data can be obtained free of charge from The Cambridge Crystallographic Data Centre via www.ccdc.cam.ac.uk/data_request/cif

■ AUTHOR INFORMATION

Corresponding Author

*Phone: (+34)976-762559. E-mail: sicilia@unizar.es.

Notes

The authors declare no competing financial interest.

■ ACKNOWLEDGMENTS

This work was supported by the Spanish Ministerio de Economía y Competitividad, MINECO, (Project No. CTQ2012-35251) and the Gobierno de Aragón (Grupo Consolidado E21: Química Inorgánica y de los Compuestos Organometálicos). The authors are grateful to the Instituto de Biocomputación y Física de Sistemas Complejos (BIFI) and the Centro de Supercomputación de Galicia (CESGA) for generous allocation of computational resources. P.B. acknowledges the support of a FPI grant from the Spanish government. M.B. acknowledges the Universidad de Zaragoza for financial support (Project No. UZ2014-CIE-01). We thank Dr. J. Pelayo and Dr. J. M. Casas (Univ. of Zaragoza) for their help with green LEDs and Dr. B. Menjón (CSIC) for helpful discussions. The referees of this work have provided an extraordinary number of helpful suggestions for improvement. V.S. thanks these anonymous colleagues for their careful reading.

■ DEDICATION

Dedicated to Dr. Babil Menjón on the occasion of his 55th birthday.

■ REFERENCES

- (1) Collman, J. P.; Hegedus, L. S.; Norton, J. R.; Finke, R. G. *Principles and Applications of Organotransition Metal Chemistry*; University Science Books: Mill Valley, CA, 1987.
- (2) Crabtree, R. H. *Organometallic Chemistry of the Transition Metals*, 3rd ed.; John Wiley & Sons: New York, 2001.
- (3) Atwood, J. D. *Inorganic and Organometallic Reaction Mechanisms*, 2nd ed.; Wiley-VCH: Weinheim, Germany, 1997.
- (4) Venter, J. A.; Leipoldt, J. G.; van Eldik, R. *Inorg. Chem.* **1991**, *30*, 2207.
- (5) Collman, J. P.; Brauman, J. I.; Madonik, A. L. *Organometallics* **1986**, *5*, 310.
- (6) Labinger, J. A.; Osborn, J. A.; Coville, N. J. *Inorg. Chem.* **1980**, *19*, 3236.
- (7) Skinner, C. E.; Jones, M. M. *J. Am. Chem. Soc.* **1969**, *91*, 4405.
- (8) van Beek, J. A. M.; van Koten, G.; Wehman-Ooyevaar, I. C. M.; Smeets, W. J. J.; van der Sluis, P.; Spek, A. L. *J. Chem. Soc., Dalton Trans.* **1991**, 883.
- (9) van Beek, J. A. M.; van Koten, G.; Smeets, W. J. J.; Spek, A. L. *J. Am. Chem. Soc.* **1986**, *108*, 5010.
- (10) Safa, M.; Puddephatt, R. J. *J. Organomet. Chem.* **2013**, *724*, 7.
- (11) Nabavizadeh, S. M.; Amini, H.; Rashidi, M.; Pellarin, K. R.; McCready, M. S.; Cooper, B. F. T.; Puddephatt, R. J. *J. Organomet. Chem.* **2012**, *713*, 60.
- (12) Bonnington, K. J.; Jennings, M. C.; Puddephatt, R. J. *Organometallics* **2008**, *27*, 6521.
- (13) Canty, A. J.; Gardiner, M. G.; Jones, R. C.; Rodemann, T.; Sharma, M. J. *Am. Chem. Soc.* **2009**, *131*, 7236.
- (14) Fackler, J. P. *Inorg. Chem.* **2002**, *41*, 6959.
- (15) Gray, T. G.; Veige, A. S.; Nocera, D. G. *J. Am. Chem. Soc.* **2004**, *126*, 9760.
- (16) Powers, D. C.; Benitez, D.; Tkatchouk, E.; Goddard, W. A., III; Ritter, T. *J. Am. Chem. Soc.* **2010**, *132*, 14092.
- (17) Powers, D. C.; Geibel, M. A. L.; Klein, J. E. M. N.; Ritter, T. *J. Am. Chem. Soc.* **2009**, *131*, 17050.
- (18) Powers, D. C.; Lee, E.; Ariafard, A.; Sanford, M. S.; Yates, B. F.; Canty, A. J.; Ritter, T. *J. Am. Chem. Soc.* **2012**, *134*, 12002.
- (19) Oro, L. A.; Sola, E.; López, J. A.; Torres, F.; Elduque, A.; Lahoz, F. *J. Inorg. Chem. Commun.* **1998**, *1*, 64.
- (20) Fjeldsted, D. O. K.; Stobart, S. R.; Zaworotko, M. J. *J. Am. Chem. Soc.* **1985**, *107*, 8258.
- (21) Atwood, J. L.; Beveridge, K. A.; Bushnell, G. W.; Dixon, K. R.; Eadie, D. T.; Stobart, S. R.; Zaworotko, M. J. *Inorg. Chem.* **1984**, *23*, 4050.
- (22) Casado, M. A.; Pérez-Torrente, J. J.; Ciriano, M. A.; Dobrinovitch, I. T.; Lahoz, F. J.; Oro, L. A. *Inorg. Chem.* **2003**, *42*, 3956.
- (23) Kalck, P.; Bonnet, J.-J. *Organometallics* **1982**, *1*, 1211.
- (24) Kolel-Veetil, M. K.; Rheingold, A. L.; Ahmed, K. J. *Organometallics* **1993**, *12*, 3439.
- (25) Schenck, T. G.; Milne, C. R. C.; Sawyer, F. J.; Bosnich, B. *Inorg. Chem.* **1985**, *24*, 2338.
- (26) Ciriano, M. A.; Pérez-Torrente, J. J.; Oro, L. A. *J. Organomet. Chem.* **1993**, *445*, 273.
- (27) Caspar, J. V.; Gray, H. B. *J. Am. Chem. Soc.* **1984**, *106*, 3029.
- (28) Tejell, C.; Ciriano, M. A.; López, J. A.; Lahoz, F. J.; Oro, L. A. *Organometallics* **2000**, *19*, 4977.
- (29) Mena, I.; Jaseer, E. A.; Casado, M. A.; García-Orduña, P.; Lahoz, F. J.; Oro, L. A. *Chem. - Eur. J.* **2013**, *19*, 5665.
- (30) Tejell, C.; Ciriano, M. A.; Edwards, A. J.; Lahoz, F. J.; Oro, L. A. *Organometallics* **1997**, *16*, 45.
- (31) Jamali, S.; Nabavizadeh, S. M.; Rashidi, M. *Inorg. Chem.* **2008**, *47*, 5441.
- (32) Nabavizadeh, S. M.; Aseman, M. D.; Ghaffari, B.; Rashidi, M.; Hosseini, F. N.; Azimi, G. *J. Organomet. Chem.* **2012**, *715*, 73.
- (33) Nabavizadeh, S. M.; Sepehrpour, H.; Kia, R.; Rheingold, A. L. *J. Organomet. Chem.* **2013**, *745–746*, 148.
- (34) Jamali, S.; Nabavizadeh, S. M.; Rashidi, M. *Inorg. Chem.* **2005**, *44*, 8594.
- (35) Che, C.-M.; Schaefer, W. P.; Gray, H. B.; Dickson, M. K.; Stein, P. B.; Roundhill, D. M. *J. Am. Chem. Soc.* **1982**, *104*, 4253.
- (36) Roundhill, D. M.; Gray, H. B.; Che, C. M. *Acc. Chem. Res.* **1989**, *22*, 55.
- (37) Bellitto, C.; Flamini, A.; Gastaldi, L.; Scaramuzza, L. *Inorg. Chem.* **1983**, *22*, 444.
- (38) Bennett, M. A.; Bhargava, S. K.; Cheng, E. C. C.; Lam, W. H.; Lee, T. K. M.; Privér, S. H.; Wagler, J.; Willis, A. C.; Yam, V. W. W. *J. Am. Chem. Soc.* **2010**, *132*, 7094.
- (39) Sicilia, V.; Fornies, J.; Casas, J. M.; Martín, A.; López, J. A.; Larraz, C.; Borja, P.; Ovejero, C.; Tordera, D.; Bolink, H. *Inorg. Chem.* **2012**, *51*, 3427.
- (40) Sicilia, V.; Borja, P.; Casas, J. M.; Fuertes, S.; Martín, A. *J. Organomet. Chem.* **2013**, *731*, 10.
- (41) Bennett, M. A.; Bhargava, S. K.; Bond, A. M.; Edwards, A. J.; Guo, S.-X.; Privér, S. H.; Rae, A. D.; Willis, A. C. *Inorg. Chem.* **2004**, *43*, 7752.
- (42) Umakoshi, K.; Kinoshita, I.; Ichimura, A.; Ooi, S. *Inorg. Chem.* **1987**, *26*, 3551.
- (43) Koshiyama, T.; Omura, A.; Kato, M. *Chem. Lett.* **2004**, *33*, 1386.
- (44) Roundhill, D. M.; Dickson, M. K.; Atherton, S. J. *J. Organomet. Chem.* **1987**, *335*, 413.
- (45) Aoki, R.; Kobayashi, A.; Chang, H.; Kato, M. *Bull. Chem. Soc. Jpn.* **2011**, *84*, 218.
- (46) Díez, A.; Fornies, J.; Larraz, C.; Lalinde, E.; López, J. A.; Martín, A.; Moreno, M. T.; Sicilia, V. *Inorg. Chem.* **2010**, *49*, 3239.
- (47) Holland, L.; Shen, W.-Z.; von Grebe, P.; Sanz Miguel, P. J.; Pichierri, F.; Springer, A.; Schalley, C. A.; Lippert, B. *Dalton Trans.* **2011**, *40*, 5159.
- (48) Janiak, C. *J. Chem. Soc., Dalton Trans.* **2000**, 3885.
- (49) Petersen, A. R.; Taylor, R. A.; Vicente-Hernández, I.; Mallender, P. R.; Olley, H.; White, A. J. P.; Britovsek, G. J. P. *J. Am. Chem. Soc.* **2014**, *136*, 14089.
- (50) Boisvert, L.; Denney, M. C.; Hanson, S. K.; Goldberg, K. I. *J. Am. Chem. Soc.* **2009**, *131*, 15802.
- (51) Grice, K. A.; Goldberg, K. I. *Organometallics* **2009**, *28*, 953.
- (52) Taylor, R. A.; Law, D. J.; Sunley, G. J.; White, A. J. P.; Britovsek, G. J. P. *Angew. Chem., Int. Ed.* **2009**, *48*, 5900.

- (53) Monomeric Pt(II) and Pt(IV) methoxide complexes typically show $^3J_{\text{Pt-H}}$ values of ca. 20–60 Hz in the ^1H NMR spectrum.
- (54) Safa, M.; Jennings, M. C.; Puddephatt, R. J. *Organometallics* **2011**, *30*, 5625.
- (55) Pellarin, K. R.; Puddephatt, R. J. *Organometallics* **2013**, *32*, 3604.
- (56) Rostovtsev, V. V.; Labinger, J. A.; Bercaw, J. E.; Lasseter, T. L.; Goldberg, K. I. *Organometallics* **1998**, *17*, 4530.
- (57) Scollard, J. D.; Day, M.; Labinger, J. A.; Bercaw, J. E. *Helv. Chim. Acta* **2001**, *84*, 3247.
- (58) Appleton, T. G.; D'Alton, C. J.; Hall, J. R.; Mathieson, M. T.; Williams, M. A. *Can. J. Chem.* **1996**, *74*, 2008.
- (59) Ferguson, G.; Monaghan, P. K.; Parvez, M.; Puddephatt, R. J. *Organometallics* **1985**, *4*, 1669.
- (60) In the air, 33% of **3d** was transformed into **2c**, in the sample containing Gal^\bullet , while only 20% was transformed in the absence of Gal^\bullet . Under Ar atmosphere, 20% of **3d** was transformed into **2c** in the sample containing Gal^\bullet , while no transformation was observable in the absence of Gal^\bullet .
- (61) van Slageren, J.; Klein, A.; Zalis, S. *Coord. Chem. Rev.* **2002**, *230*, 193.
- (62) Vogler, A.; Kunkely, H. *Inorg. Chem.* **1982**, *21*, 1172.
- (63) Hoggard, P. E.; Vogler, A. *Inorg. Chim. Acta* **2003**, *348*, 229.
- (64) Hoggard, P. E.; Bridgeman, A. J.; Kunkely, H.; Vogler, A. *Inorg. Chim. Acta* **2004**, *357*, 639.
- (65) Whang, S.; Estrada, T.; Hoggard, P. E. *Photochem. Photobiol.* **2004**, *79*, 356.
- (66) Von Zelewsky, A.; Suckling, A. P.; Stoeckli-Evans, H. *Inorg. Chem.* **1993**, *32*, 4585.
- (67) The nature of **3a** was established by comparison of its ^1H NMR signals with those of **3b–3d** in the low-field region of the spectrum.
- (68) Hill, R. H.; Puddephatt, R. J. *J. Am. Chem. Soc.* **1985**, *107*, 1218.
- (69) Morrison, R. T.; Boyd, R. N. *Química Orgánica*, 5th ed.; Pearson Educación: México, 1998.
- (70) Holleman, A. F.; Wiberg, E. *Inorganic Chemistry*, Academic Press: Berlin, 1995.
- (71) Xie, J.; Otto, R.; Mikosch, J.; Zhang, J.; Wester, R.; Hase, W. L. *Acc. Chem. Res.* **2014**, *47*, 2960.